다수의 바퀴를 가진 차량의 동적 거동 해석의 수학적 모델

김준영*

한국해양대학교 조선기자재공학부

Mathematical Model for Dynamic Performance Analysis of Multi-Wheel Vehicle

Joon-Young Kim*

Division of Maritime Equipment Engineering, Korea Maritime University

요 약 본 연구에서 모사 프로그램이 6WD/6WS를 가진 특수 목적 차량의 비정상상태 코너링 성능을 조사하기 위해 개발되었다. 6WD 차량은 비포장 도로에서 작전을 수행하기 좋은 성능을 가지고 있고 안전한 성능을 가진 것으로 신뢰받고 있다. 그러나, 6WS 차량들의 코너링 성능은 관련 문헌을 통해서는 언뜻 이해가 어렵다. 본 논문에서는 6WD/6WS 차량들은 비선형 차량 동력학, 타이어 모델, 운동학적 효과 등을 포함한 18 자유도 시스템으로 모델링 되었다. 그리고 그 차량 모델은 입/출력과 차량변수가 수식화된 접근 방법으로 쉽게 변환될 수 있도록 MATLAB/SIMULINK를 사용한 모사 프로그램으로 구성되었다. 6WS 차량의 코너링 성능은 브레이크 휠과 피봇팅 각각으로 해석되었다. 모사 결과들을 보면, 코너링 성능은 전후 휠 조향 뿐만이 아니라 중간 휠 조향에 따라 좌우됨을 보여준다. 덧붙여, 새로운 6WS 제어법칙은 측면 미끄러짐 각을 최소화하기 위해 제안되었다. 차량변경 모사 결과들은 제안된 제어법칙의 6WS 차량의 장점을 보여준다.

• **주제어** : 6더블유디/6더블유에스 자동차, 수학모델, 코너링 성능, 6더블유에스 제어법

Abstract In this study, a simulation program is developed in order to investigate non steady-state cornering performance of 6WD/6WS special-purpose vehicles. 6WD vehicles are believed to have good performance on off-the-road maneuvering and to have fail-safe capabilities. But the cornering performances of 6WS vehicles are not well understood in the related literature. In this paper, 6WD/6WS vehicles are modeled as a 18 DOF system which includes non-linear vehicle dynamics, tire models, and kinematic effects. Then the vehicle model is constructed into a simulation program using the MATLAB/SIMULINK so that input/output and vehicle parameters can be changed easily with the modulated approach. Cornering performance of the 6WS vehicle is analyzed for brake steering and pivoting, respectively. Simulation results show that cornering performance depends on the middle-wheel steering as well as front/rear wheel steering. In addition, a new 6WS control law is proposed in order to minimize the sideslip angle. Lane change simulation results demonstrate the advantage of 6WS vehicles with the proposed control law.

• **Key Words** : 6WD/6WS Vehicle, Mathematical Model, Cornering Performance, 6WS Control Law

*교신저자 : 김준영(jykim@hhu.ac.kr)

접수일 2012년 9월 1일 수정일 2012년 11월 25일 게재확정일 2012년 11월 30일

1. Introduction

Multi-wheel drive vehicles applied in special environments are believed to have more tractive force, better steerability and stability. Some of the vehicles have middle wheels under the center section of the hull and are named 6WD/6WS (6-wheel-drive/ 6-wheel-steering) vehicles. These 6WD/6WS vehicles are known to have sufficient structural stability because of the load distribution, and thus, to minimize the tendency of pitching during abrupt braking or acceleration. Because 6WD vehicles can possess better traction and braking capability than 2WD or 4WD vehicles, they can accelerate or brake better on off-the-road and they can continue to move when one or two of their tires are blown off or there are transverse rigid-type obstacles. However, the performance of 6WS (6-wheel-steering) vehicles which are believed to have better maneuverability than 2WS or 4WS vehicles are not quite understood in the related literature.

Although 4WS vehicles have been extensively studied and their results can be extended to 6WS vehicles, few results are reported about the coordination among six wheel steerings.

In this paper, coordination between six wheel steerings are extensively investigated for the cornering performance analysis. 6WD/6WS vehicles are modeled as a 18 DOF system which includes 12 DOF nonlinear vehicle dynamics, 6 DOF wheel dynamics, tire model and kinematic effects. This model is constructed into a simulation program using MATLAB/SIMULINK and its cornering performance is evaluated with the various steering coordination. Simulations are executed for cornering combined with braking and pivoting, respectively. In order to minimize the sideslip angle during lane change, a new 6WS control law is proposed and its results are compared to conventional 4WS control laws.

Research on vehicle dynamics and simulations has grown enormously, from simulations of high-order models with all kinds of non-linearities to simulations and controls of linear bicycle models. Smith and Starkey[1] studied the relationship between model complexity and simulation accuracy with three different vehicle models and concluded that linear models are not suitable at high g's maneuvering. Nalecz and Bindermann[2] utilized a 3 DOF model including suspension and steering systems, and they demonstrated that roll steer and lateral weight transfer were crucial factors in cornering performance. Xia and Law[3] compared various 4WS control algorithms based on a nonlinear 8 DOF model with kinematic effects. Abe[4] proposed a 4WS control law in order to minimize the sideslip angle using a linear 2 DOF model.

Tire models which are essential for vehicle dynamics study have been investigated actively. Examples of the proposed models are theoretical models based on friction ellipse[5] and empirical models based on experimental data[6, 7 and 8].

In commercial vehicles research, characteristics of heavy vehicles are considered different from passenger ones because of the increased weight and number of wheels. Pillar and Braun[9] implemented various steering algorithms on multi-wheeled heavy trucks. Das et al.[10] derived a dynamic model of heavy trucks and executed simulations for stability and maneuvering study. Hata et al.[11] experimented medium-duty truck with 4WS and investigated controllability and stability.

Studies on 6-wheeled vehicles have been concentrated on armored vehicles because they are favored by military operations[12]. Examples of 6-wheeled armored vehicles are; M38 made in U.S.A, Alvis Saladin in Britain; and Gendron Somua in France. Those 6-wheeled vehicles adopted independent suspensions and all-wheel-drive systems in order to have comparable off-the-road performance as tracked vehicles do. The implemented prototypes are reported that off-the-road performance of the 6-wheeled vehicles were adequate except on clay soils and they were also able to pivot like tracked vehicles[13].

2. 6WD/6WS Vehicle Model

6WD/6WS vehicle considered in this paper consists of six 30 hp electric motors, electrically controlled steering, and 5 ton weights. It has a sprung mass and six unsprung masses and independent suspensions. The detailed description of the vehicle is listed in Table 1. The dynamic characteristics of the vehicle is modeled based on the following assumptions:

Longitudinal, lateral, vertical, rolling, pitching, and yawing motion are considered.

Vertical motion of the unsprung mass is identical to the z-direction of vehicle-fixed axis.

Vertical motion of the sprung mass is transferred through the suspension.

The longitudinal and the lateral load transfer is considered.

Kinematic effects such as roll steer, camber angle and tire side force lag are considered.

[Table 1] Vehicle Parameters

Vehicle mass	M	5000 kg
Unsprung mass	m	190 kg
Moment of inertia (X Axis)	I_x	3619.5 kgm^2
Moment of inertia (Y Axis)	I_y	12306.5 kgm^2
Moment of inertia (Z Axis)	I_z	14478 kgm^2
Distance from c.g. to front axle	l_f	1.8 m
Distance from c.g. to middle axle	l_m	0.2 m
Distance from c.g. to rear axle	l_r	2.2 m
Distance from c.g. to round	h	1.25 m
Track width	2d	3 m
Spring coefficient of suspension	k	89266 N/m
Damping coefficient of suspension	b	1762.5 Ns/m
Spring coefficient of the tire	K_t	682960 N/m
Roll bar stiffness	K_r	2566 Nm/rad
Rotating wheel inertia	I_ω	6.25 kgm^2
Tire radius	r_w	0.5 m
Nominal longitudinal stiffness	C_s	168118 N/skid
Nominal cornering stiffness	C_α	112078 N/rad
Friction coefficient	μ	0.6
Road adhesion reduction factor	ε_r	0.015 s/m
Front roll steer coefficient	K_{rsf}	0.15
Middle roll steer coefficient	K_{rsm}	0.15
Rear roll steer coefficient	K_{rsr}	0.15
Lateral force lag time coefficient	C_{tl}	1
Ratio of camber angle to roll angle	K_γ	0.1

2.1 Vehicle Dynamics model

Fig. 1 shows a body-fixed coordinate system of the 6-wheeled vehicle. Fig. 2 shows the suspension linked with each tires. Wheel rotation model in side view is shown in Fig. 3 and all the variables are explained in Nomenclature and Table 1.

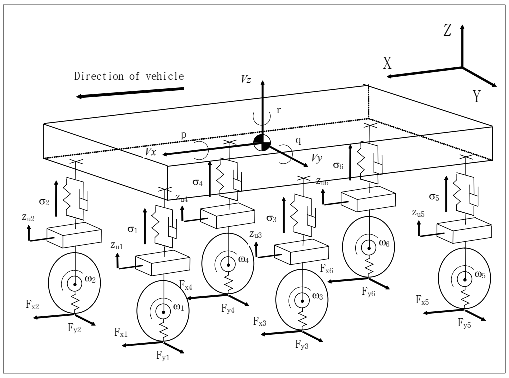

[Fig. 1] Body-Fixed Coordinate System

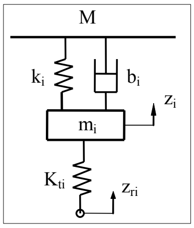

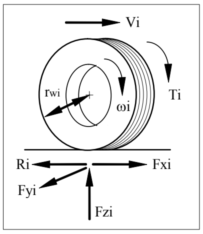

[Fig. 2] Suspension System [Fig. 3] Wheel Rotation

Based on the above assumptions and coordinates the vehicle is modeled into the following 18 DOF system.

longitudinal : $M \cdot (\dot{V}_x + V_z \cdot q - V_y \cdot r) = F_x$ (1)

lateral : $M \cdot (\dot{V}_y + V_x \cdot r - V_z \cdot p) = F_y$ (2)

vertical : $M \cdot (\dot{V}_z + V_y \cdot p - V_x \cdot q) = F_z$ (3)

rolling : $I_x \cdot \dot{p} + (I_z - I_y) \cdot q \cdot r = M_x$ (4)

pitching : $I_y \cdot \dot{q} + (I_x - I_z) \cdot r \cdot p = M_y$ (5)

yawing : $I_z \cdot \dot{r} + (I_y - I_x) \cdot p \cdot q = M_z$ (6)

unsprung mass motion :(i=1~6),

$$m_i \cdot \ddot{z}_i = -F_{si} + K_{ti} \cdot (z_{ri} - z_i) + (-1)^{i+1} \frac{K_{ri} \cdot \varnothing}{2d} \quad (7)$$

wheel rotation:

$$\dot{\omega}_i = \frac{1}{I_{Wi}} \cdot (T_i - r_{Wi} \cdot F_{xi} + r_{Wi} \cdot R_i) \quad (8)$$

where F_x and F_y are resultant forces about x-axis and y-axis, respectively. These forces are expressed as the tire force, rolling resistance and aerodynamic drag. Fz is expressed as resultant forces by road input of the tire and suspension force named Fs. Mx, My, and Mz are resultant moments about x-axis, y-axis, and z-axis, respectively. Expressions for these variable are omit for the simplicity of the paper.

2.2 Tire model

Because vehicle tires generate the traction and the lateral force contacted with the terrain, they are the most difficult components for the vehicle modeling accompanied with nonlinearities. In this study, Dugoff's model [5] where tire forces are expressed as the slip angle and the slip ratio is introduced. The longitudinal and the lateral force at i-th wheel are expressed as

$$F_{xi} = \frac{C_s \cdot s_i}{1 - s_i} \cdot X_i \cdot (2 - X_i) \tag{9}$$

$$F_{yi} = \frac{C_\alpha \cdot \tan\alpha_i}{1 - s_i} \cdot X_i \cdot (2 - X_i) \tag{10}$$

$$S_i = \begin{cases} \dfrac{r_W \omega_i - V_i}{r_W \omega_i} \ \text{if} \ r_W \omega_i \le V_i \quad (\in acceleration) \\ \dfrac{V_i - r_W \omega_i}{V_i} \ \text{if} \ r_W \omega_i > V_i \quad (\in braking) \end{cases} \tag{11}$$

$$X_i = \begin{cases} X_i & \text{if} \ X_i \le 1 \\ 1 & \text{if} \ X_i > 1 \end{cases} \tag{12}$$

$$X_i = \frac{\mu_i \cdot F_{zi} \cdot (1 - s_i) \cdot (1 - \epsilon_r \cdot V_i \cdot \sqrt{s_i^2 + \tan^2\alpha_i})}{2\sqrt{C_s^2 \cdot s_i^2 + C_\alpha^2 \cdot \tan^2\alpha_i}} \tag{13}$$

where X_i means the non-dimensional total slip coefficient considering the slip angle and the slip ratio. It becomes the value of 1 when there is no sliding between the tires and the road. In order to minimize the sliding of the tires, it is necessary to keep the value of X_i large. If the sliding occurs excessively, the value of Xi is approaching zero and the tire force becomes very small. Fzi is the vertical force considering the longitudinal and the lateral weight transfer.

3. Simulation Program

The 6WD/6WS vehicle model derived in the previous section is constructed into a simulation program using the MATLAB/ SIMULINK. Fig. 4 shows a simulink model of the overall system and each block is composed of hierarchical sub-blocks.

For the convenience of the user, frequently-used commands are built into the command blocks.

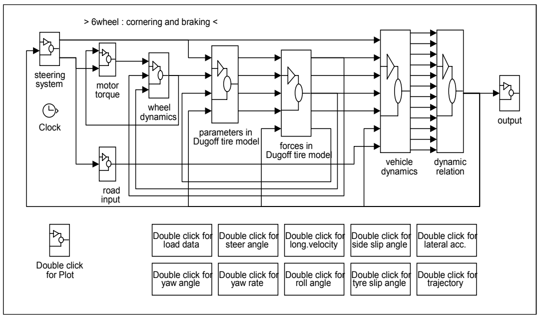

[Fig. 4] Simulink Model

Inputs to the model are; steer angles from the driver and steering control laws; drive/brake torques from the motors and brakes; and road input on running. The motor torque block can select a engine module or a motor module, by which the power source of the vehicle can be a combustion engine or electric motors. The vehicle dynamics block consists of the longitudinal, lateral, vertical, rolling, pitching, and yawing sub-blocks. Dugoff tire model block produces the tractive/braking and side forces at each wheel. Outputs from the model calculates the state variables such as the vehicle velocity, yaw rate, sideslip angle, etc.

4. Simulation Results

The considered vehicle is 5 ton weight similar to medium-duty trucks and is driven by six 30hp AC motors with the gear ratio of 5:1. The motor torque is assumed constant in 0~2400 rpm range and inversely proportional to the motor speed over 2400 rpm.

In order to investigate the coordination between the six wheel steerings of the 6WS vehicles, 5 different steering modes are considered as shown in Fig. 5. For the simplicity of the comparison, the middle and the rear wheel steer angles are chosen form 0° or ±2° and the front wheel steer angle is fixed to 4° in this section. However, in the next section, a new six wheel steering control law is proposed and its cornering performance is evaluated.

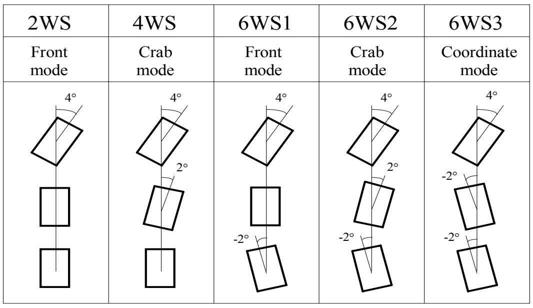

[Fig. 5] Five Different Steering Modes

4.1 Frequency Response Analysis

Based on the 2 DOF linear model in Fig. 6 frequency response analysis is carried out for comparing the five steering modes in Fig. 5. Assuming a constant speed of 80 km/h, the lateral acceleration and the yaw rate responses are compared in Fig. 7 and Fig. 8, respectively.

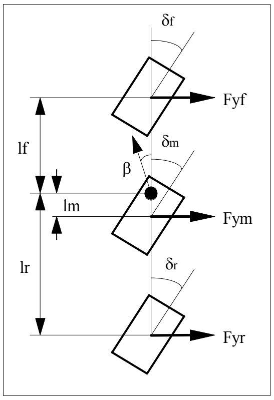

[Fig. 6] 2DOF Vehicle Model

The lateral acceleration and the yaw rate frequency responses show the characteristics of a low-pass filter. That is, as the frequency of the steering input is increased, the response gain is decreased with the increased phase lag. The lateral acceleration response shows that the gains of the 6WS vehicles are larger than the others but the phase lag of the 4WS vehicle is the smallest. The yaw rate response shows that the gains of the 6WS vehicles are the largest and the phase lag of the 6WS3 is the smallest. According to this analysis, it can be concluded that 6WS3, the coordinate mode of 6WS, is the best choice with the fast yawing motion but pays large lateral acceleration.

Because the linear model used here assumes that the mass center is located a little forward from the vehicle center, the effect of rear wheel steering is large compared to that of the middle wheel steering. But in the next section the 18 DOF model will clearly show the effect of the middle wheel steering.

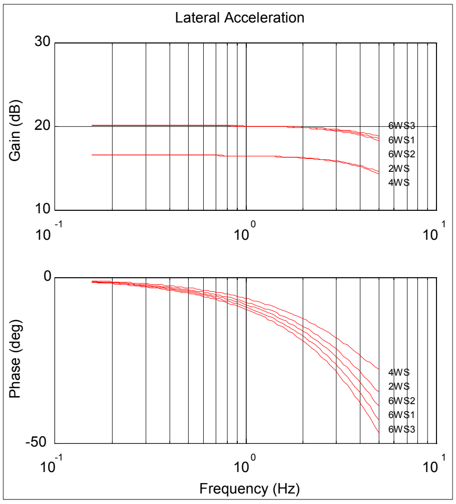

[Fig. 7] Lateral Acceleration Frequency Response

4.2 Braking steering

Braking while steering is a very common maneuver and its cornering performance is investigated based on the 18 DOF vehicle model introduced in vehicle model section. While the vehicle is driving at 72 km/h, the brake torque is applied at each wheel and the steering is started from 0.5 second. The steer angle is increased and fixed into each steering mode listed in Fig. 5. Because the road condition is assumed not-paved, the friction coefficient is set to a value of 0.6.

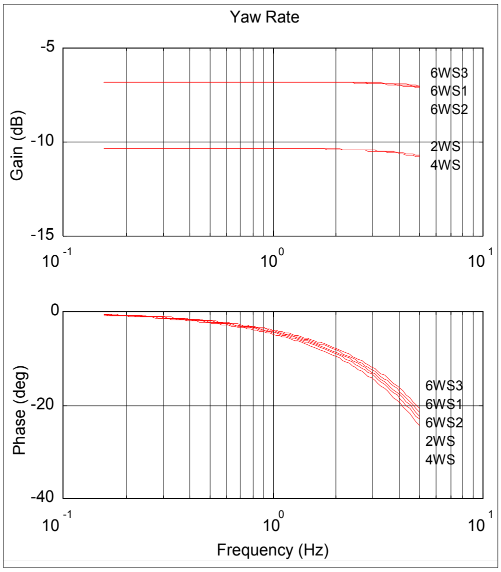

[Fig. 8] Yaw Rate Frequency Response

Simulation results for the five steering modes in Fig. 5 are compared with respect to the lateral acceleration [Fig. 9], yaw rate [Fig. 10], sideslip angle [Fig. 11] and trajectory [Fig. 12]. In general, 6WS modes have larger lateral acceleration, yaw rate, sideslip angle and smaller turning radius than 2WS and 4WS modes. Among 6WS modes, 6WS2 (crab-mode middle-wheel steering) gives the smallest turning radius with a large sideslip angle. This cornering difference, in particular, the influence of the middle wheel steering is caused by the nonlinear tire model and the weight transfer in the vehicle model.

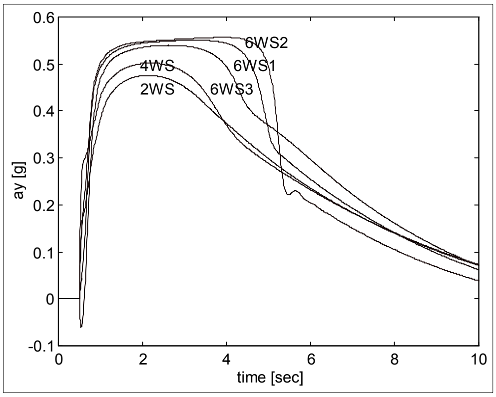

[Fig. 9] Lateral Acceleration

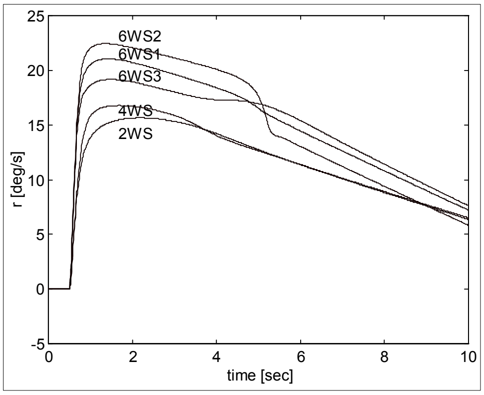

[Fig. 10] Yaw Rate

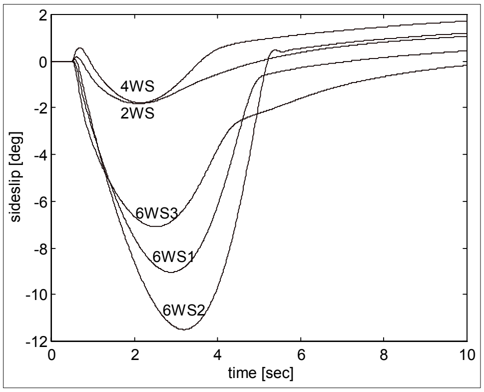

[Fig. 11] Sideslip Angle

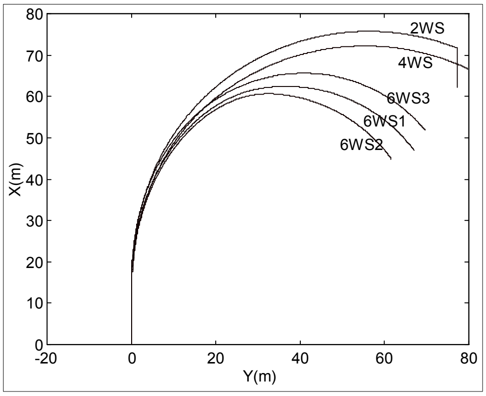

[Fig. 12] Trajectory

4.3 Pivoting

Pivoting is considered as one of the special specifications of the 6WD/6WS vehicle and its feasibility is investigated in this section. Because the electric motors are used for the traction and the steering, the direction and the orientation of the motors are assumed to be easily changed for the pivoting purpose. In order to pivot with respect to the geometrical center of the vehicle, the direction and the steer angle of the wheels should be in the form of Fig. 13. The driving torque applied to the middle wheels are smaller than the front/rear for the geometrical equilibrium. The driving torque and the braking torque are selected such that the vehicle can stop after pivoting 180 degree rotation. The pivoting trajectory and the yaw angle response are plotted in Fig. 14 and Fig. 15, respectively, and demonstrate the feasibility of pivoting similar to the tracked vehicles.

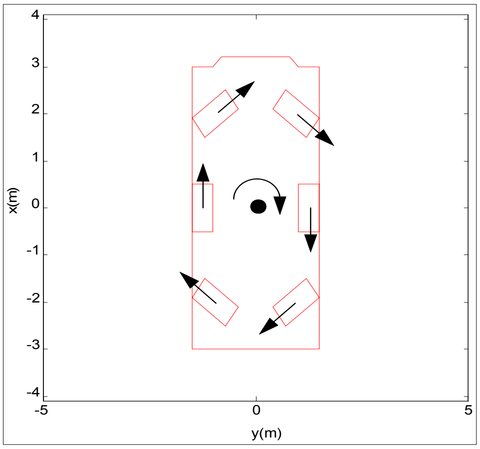

[Fig. 13] Initial State

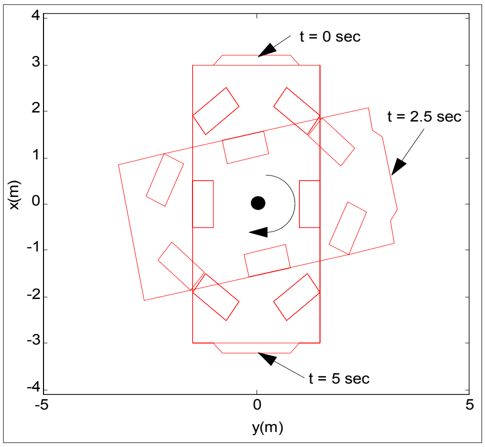

[Fig. 14] Trajectory

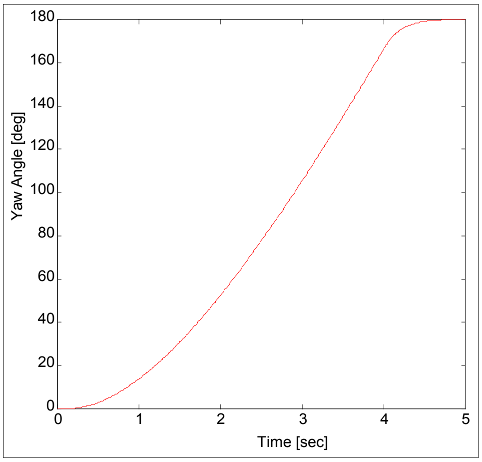

[Fig. 15] Yaw Angle

5. A proposed 6WS control law

A new 6WS control law is proposed in order to minimize the sideslip angle during lane change. As illustrated in Fig. 9 and Fig. 11, 6WS vehicles with the fixed steer angle have larger lateral acceleration and sideslip angle than 2WS and 4WS vehicles. This phenomena can be regarded as less maneuverability and less stability. To overcome this limitation, a new steering control law is developed based on the vehicle speed and the front wheel steer angle.

5.1 Vehicle model

The vehicle model used for the controller design is a linear bicycle model having 2 DOF. Based on the bicycle model in Fig. 6, the equations of motion are derived regarding the sideslip and the yaw rate.

lateral motion :

$$MV_x(\dot{\beta}+r) = 2F_{yf} + 2F_{ym} + 2F_{yr} \tag{14}$$

yawing motion :

$$I_z\dot{r} = 2l_fF_{yf} - 2l_mF_{ym} - 2l_rF_{yr} \tag{15}$$

where β is the sideslip angle, r is the yaw rate, V_x is vehicle speed and other variables are explained in the Nomenclature. Assuming that steer angles are small, the above equations can be rewritten into the following matrix form :

$$\begin{bmatrix}\dot{\beta}\\ \dot{r}\end{bmatrix}=\begin{bmatrix}\frac{-2}{MV_x}(C_f+C_m+C_r) & -1-\frac{2}{MV_x^2}(l_fC_f-l_mC_m-l_rC_r)\\ \frac{-2}{I_Z}(l_fC_f-l_mC_m-l_rC_r) & -\frac{2}{I_ZV_x}(l_f^2C_f+l_m^2C_m+l_r^2C_r)\end{bmatrix}\begin{bmatrix}\beta\\ r\end{bmatrix}$$

$$+\begin{bmatrix}\frac{2C_f}{MV_x} & \frac{2C_m}{MV_x} & \frac{2C_r}{MV_x}\\ \frac{2l_fC_f}{I_Z} & -\frac{2l_mC_m}{I_Z} & -\frac{2l_rC_r}{I_Z}\end{bmatrix}\begin{bmatrix}\delta_f\\ \delta_m\\ \delta_r\end{bmatrix} \qquad (16)$$

5.2 Control law

For a given vehicle speed and a front wheel steer angle, the middle and the rear wheels need to steered appropriately for the required maneuvering and stability. In this section, assuming that the middle-wheel steer angle is a half of the front steer angle, a steering control laws for the rear wheels is developed to minimize the sideslip angle at the mass center. Similar to 4WS cases[3 and 4], the rear wheel steer angle is assumed to depend on the vehicle speed and the front steer angle.

$$\delta_m = \frac{1}{2}\delta_f \qquad (17)$$

$$\delta_r = k_1 \bullet \delta_f \bullet k_2 \bullet r \qquad (18)$$

By substituting Eq. 17 and 18 into Eq. 16 and setting zero to the determinant of the numerator of the transfer function between δ_f and b, the following relations are obtained for k_1 and k_2.

$$k_1 = \frac{-2C_f - C_m}{2C_r} \qquad (19)$$

$$k_2 = \frac{MV_x^2 + 2(C_fl_f - C_ml_m - C_rl_r)}{2C_rV_x} \qquad (20)$$

5.3 Lane Change

In order to evaluate the above control law compared to 2WS and 4WS, a lane change maneuvering is simulated as shown in Fig. 16. The vehicle is supposed to follow the trajectory with maintaining the vehicle speed of 56 km/h. It is assumed that the front wheel is steered appropriately by a driver. In applying the existing 4WS algorithms[4] to the 6-wheeled vehicle, the middle wheel is not steered and the rear wheel is steered according to the algorithm. In the 6WS, the middle wheel is steered to a half of the front wheel steering and the rear wheel is steered according to the proposed control law as shown in Fig. 17.

4WS law [4] :

$$\delta_r = -\frac{C_f + C_m}{C_r}\delta_f + \frac{MV_x^2 + 2(C_fl_f - C_rl_r)}{2C_rV_x}r \qquad (21)$$

6WS law :

$$\delta_r = \frac{-2C_f - C_m}{2C_r}\delta_f + \frac{MV_x^2 + 2(C_fl_f - C_ml_m - C_rl_r)}{2C_rV_x}r \qquad (22)$$

where C_f, C_m, and C_r are the cornering stiffness of the front, middle and rear wheels, respectively.

Lane change results show that the proposed 6WS control law follows the desired trajectory with less steer angles than 2WS and 4WS. The lateral acceleration [Fig. 18] in 6WS case is a little smaller than 2WS and 4WS cases, but the sideslip angle [Fig. 19] in 6WS case is much smaller than the 2WS case and smaller than the 4WS case.

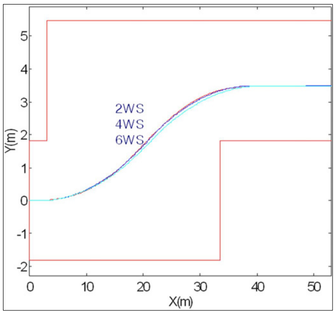

[Fig. 16] Lane Change Trajectory

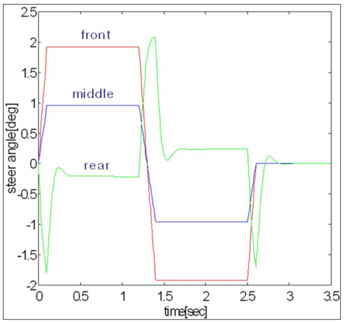

[Fig. 17] 6WS Steer Angle

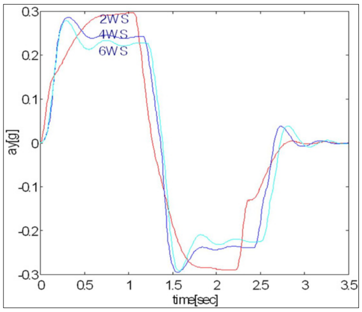

[Fig. 18] Lateral Acceleration

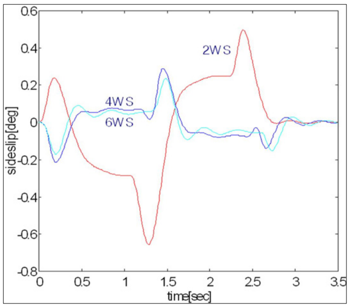

[Fig. 19] Sideslip Angle

6. Conclusions

Frequency analysis based on a 2 DOF linear model shows that 6WS vehicles have larger gain in the lateral acceleration and yaw rate than 2WS and 4WS vehicles. In order to analyze the cornering performance of 6WD/6WS vehicles, a 18 DOF nonlinear vehicle model is developed and constructed into a simulation program using the MATLAB/SIMULINK. Simulation results for the cornering combined with braking demonstrate the role of the middle wheel steering in 6WS vehicles. In particular, when the middle wheel is in the same direction with the front wheel (crab mode), the turning radius can be reduced with the increased sideslip angle. To overcome this limitation a new 6WS control law is proposed to minimize the sideslip angle. Lane change maneuvering results indicate the improved stability and maneuverability of the 6-wheeled vehicles. A feasibility study for the pivoting of the 6-wheeled vehicles is completed and illustrates the unique characteristics of the electric-driven multi-wheel vehicles.

REFERENCES

[1] D. E. Smith, J. M. Starkey, “Effects of Model Complexity on the Performance of Automated Vehicle Steering Controllers : Model Development, Validation and Comparison”, Vehicle System Dynamics, Vol. 24, pp. 163-181, 1995.

[2] A. G. Nalecz, A. C. Bindermann, “Investigation into the stability of four wheel steering vehicles”, Int. J. of Vehicle Design, Vol. 9, No. 2, pp. 159-178, 1988.

[3] X. Xia, E. H. Law, “Nonlinear Analysis of Close-Loop Driver/Automobile Performance with Four Wheel Steering Control”, SAE, 92055, 1992.

[4] M. Abe, “Handling Characteristics of Four Wheel Active Steering Vehicles over Full Maneuvering Range of Lateral and longitudinal Accelerations”, Proceedings of 11th IAVSD Symposium,Vehicle System Dynamics, Vol. 18 August 21-25, pp. 1-14, 1989.

[5] H. Dugoff, P. S. Fancher, L. Segel, “An Analysis of Tire Traction Properties and Their Influence on Vehicle Dynamic Performance”, SAE Transactions, 79:341-366, SAE Paper No. 700377, 1970.

[6] R. W. Allen, T. J. Rosenthal, H. T. Szostak, “Steady State and Transient Analysis of Ground Vehicle Handling”, SAE, 870495, 1987.

[7] E. Bakker, H. B. Pacejka, L. Lidner, “A New Tire Model with an Application in Vehicle Dynamics Studies”, SAE, 890087, 1989.

[8] L. D. Metz, “Dynamics of Four-Wheel-Steer Off-Highway Vehicles”, SAE, 930765, 1993.

[9] D. R. Pillar, E. E. Braun, “All-Wheel Steering System for Heavy Truck Application”, SAE, 952680, 1995.

[10] N. S. Das, B. A. Suresh, J. C. Wambold, “Estimation of Dynamic Rollover Threshold of Commercial Vehicles Using Low Speed Experimental Data”, SAE, 932949, 1993.

[11] N. Hata, H. Osanai, S. Hasegawa, S. Takahashi, Y. Watanabe, “An Investigation into Vehicle Controllability and Stability of an Experimental

Medium-Duty Truck with Rear-Axle Steering", AVEC, 923044, 1992.
[12] R. M. Ogorkiewicz, "Design and Development of Fighting Vehicles", Chapter10, pp.172-193, Macdonald and Co(publishers) Limited, 1968.
[13] H. Nasu and H. Higasa, "Development of yonden electric vehicle PIVOT", JSAE, Review 16, pp.77-82, 1995.

저자소개

Joon-Young Kim(김준영) **[members]**

- 1989. 2 : Inha University, Naval Architecture(B.S.)
- 1993. 2 : Inha University, Naval Architecture(M.S.)
- 1999. 2 : Hanyang University, Precision Mechanical Engineering (Ph.D)
- 2010. 2 : Korea Maritime University, Division of Marine Equipment Engineering(Professor)

<Research Parts> : Unmanned underwater vehicle design and control